

Telomeres and centromeres have interchangeable roles in promoting meiotic spindle formation

Alex Fennell,^{1,2*} Alfonso Fernández-Álvarez,^{1,2*} Kazunori Tomita,³ and Julia Promisel Cooper^{1,2}

¹Telomere Biology Section, Laboratory of Biochemistry and Molecular Biology, National Cancer Institute, National Institutes of Health, Bethesda, MD 20892

²Telomere Biology Laboratory, Cancer Research UK, London Research Institute, London WC2A 3LY, England, UK

³Chromosome Maintenance Group, UCL Cancer Institute, University College London, London WC1E 6DD, England, UK

Telomeres and centromeres have traditionally been considered to perform distinct roles. During meiotic prophase, in a conserved chromosomal configuration called the bouquet, telomeres gather to the nuclear membrane (NM), often near centrosomes. We found previously that upon disruption of the fission yeast bouquet, centrosomes failed to insert into the NM at meiosis I and nucleate bipolar spindles. Hence, the trans-NM association of telomeres with centrosomes during prophase is crucial for efficient spindle formation. Nonetheless, in approximately half of bouquet-deficient meiocytes, spindles form properly. Here, we show that bouquet-deficient cells can

successfully undergo meiosis using centromere-centrosome contact instead of telomere-centrosome contact to generate spindle formation. Accordingly, forced association between centromeres and centrosomes fully rescued the spindle defects incurred by bouquet disruption. Telomeres and centromeres both stimulate focal accumulation of the SUN domain protein Sad1 beneath the centrosome, suggesting a molecular underpinning for their shared spindle-generating ability. Our observations demonstrate an unanticipated level of interchangeability between the two most prominent chromosomal landmarks.

Introduction

Telomeres maintain the integrity of linear chromosomes by preventing the unsolicited recruitment of DNA repair machineries to chromosome ends (de Lange, 2009; Dehé and Cooper, 2010; Jain and Cooper, 2010) and engaging telomerase to solve the end replication problem (Greider and Blackburn, 1985; Artandi and Cooper, 2009). At a distinct site on the chromosome, centromeres mediate the attachment of chromosomes to spindle microtubules in specific orientations that allow accurate chromosome segregation (Cheeseman and Desai, 2008; Watanabe, 2012). Despite these separate functions, telomeres and centromeres share several similarities. Both direct the assembly of specific nucleoprotein complexes and both, as a consequence of their underlying repetitive DNA sequences, are packaged into heterochromatin (Karpen and Allshire, 1997; Stimpson and Sullivan, 2010).

Meiosis ensures the correct distribution of chromosomes from diploid progenitor cells to haploid gametes by incorporating two sequential nuclear divisions (meiosis I [MI] and II [MII]) after only a single round of DNA replication (Petronczki

et al., 2003; Yanowitz, 2010). A widely conserved feature of meiotic prophase is formation of the telomere bouquet in which telomeres gather to a confined region of the nuclear membrane (NM), often near the centrosome (Chikashige et al., 1994; Chikashige et al., 1997; Scherthan, 2001). The bouquet stage is particularly well characterized in fission yeast. During mitotic interphase, telomeres localize to two or three clusters around the NM, whereas centromeres form a single cluster beneath the centrosome, which in fission yeast is called the spindle pole body (SPB) and is located on the cytoplasmic surface of the NM. This clustering requires interactions between centromeres and the SUN domain inner NM protein Sad1 (Hagan and Yanagida, 1995; Nabetani et al., 2001; Hou et al., 2012). Sad1 interacts with the outer NM KASH domain protein Kms1, which in turn contacts the SPB. Upon meiotic induction, the meiosis-specific proteins Bqt1 and Bqt2 interact with Rap1 (a partner of the telomeric dsDNA binding protein, Taz1) and recruit Sad1-Kms1 to the distally located telomeres (Chikashige et al., 2006). Kms1 interacts with cytoplasmic dynein, forming

*A. Fennell and A. Fernández-Álvarez contributed equally to this paper.

Correspondence to Julia Promisel Cooper: julie.cooper@nih.gov

Abbreviations used in this paper: GBP, GFP-binding protein; MI, meiosis I; NM, nuclear membrane; SKS, SUN-KASH-SPB; SPB, spindle pole body.

This article is distributed under the terms of an Attribution-Noncommercial-Share Alike-No Mirror Sites license for the first six months after the publication date (see <http://www.rupress.org/terms>). After six months it is available under a Creative Commons License (Attribution-Noncommercial-Share Alike 3.0 Unported license, as described at <http://creativecommons.org/licenses/by-nc-sa/3.0/>).

a telomere–Bqt–Sad1–Kms–dynein bridge dubbed the telocentrosome, as it nucleates cytoplasmic microtubules that provide tracks for the movement of telomeres to the SPB (Yoshida et al., 2013). As telomeres accumulate beneath the SPB during bouquet formation, the centromeres are released from this site (Asakawa et al., 2005; Klutstein et al., 2015). Hence, centromeres and telomeres sequentially interact with the SPB in a cell cycle–dependent manner.

Bouquet formation is followed by the onset of dramatic oscillatory movements of the SPB that pull the telomere-led chromosomes back and forth, generating the elongated horsetail nucleus (Ding et al., 1998). At the end of prophase, the SPB settles in the middle of the cell and the telomeres dissociate from the bouquet in a concerted fashion dubbed telomere fireworks (Tomita and Cooper, 2007). This marks a critical stage for the SPB: it must complete duplication while remaining anchored to the cytoplasmic surface of the NM; mother and daughter SPBs then insert into the NM to nucleate the spindles that orchestrate MI and MII. It is at this stage that SPB behavior fails in bouquet-deficient (*taz1Δ*, *rap1Δ*, or *bqt1Δ*) cells, 50% of which display SPBs that fail to nucleate spindles (Tomita and Cooper, 2007).

Here we explore the low penetrance of spindle defects in the absence of the telomere bouquet; how is spindle formation achieved without prior contact between telomeres and the SPB? Strikingly, we find that bouquet-deficient cells can successfully undergo meiosis using centromeres instead of telomeres to generate spindle formation. Our observations indicate a surprising level of telomere–centromere interchangeability.

Results

Sporadic centromere-mediated chromatin–SPB contacts during prophase rescue *bqt1Δ* spindle defect

To address the low penetrance of spindle defects in bouquet-deficient meiosis, we examined the properties of those *bqt1Δ* meiocytes that succeed in meiotic spindle formation. In bouquet-deficient settings, the fluctuating SPB lacks stable contact with chromatin, preventing the chromosome oscillations that generate the horsetail nuclear shape (Fig. 1 A and Video 1; Chikashige et al., 2006; Tomita and Cooper, 2007). Nonetheless, we noticed that the SPB often appears to catch a chromatin segment as it passes through the static chromatin mass, generating a streak that emanates from the main bulk of chromatin (Fig. 1, B and C; and Video 2). Remarkably, although cells lacking visible chromatin–SPB contact tend to sustain spindle formation defects, those with visible chromatin–SPB contacts during meiotic prophase are significantly more likely to form robust bipolar spindles at MI despite the absence of the bouquet (Figs. 1 D and S1, A–D).

To further define the correlation between *bqt1Δ* chromatin–SPB contacts and proper spindle formation, we allocated cells into categories according to the longevity of their longest contact (see Fig. S1 and Materials and methods), ranging from <5-min chromatin–SPB contact (i.e., “no apparent contact”) to “throughout” contacts that span the entirety of prophase. This analysis

reveals a clear correlation between the longevity of prophase chromatin–SPB contacts and the recovery of *bqt1Δ* MI spindle formation (Fig. 1 D). Indeed, instances of bipolar spindle formation with no apparent contact are likely a result of contacts whose durations are shorter than the intervals between time-lapse images, as their frequency is reduced from 45% to 29% when the intervals between time-lapse images are reduced from 10 to 5 min.

During azygotic meiosis, in which stable diploids enter meiosis upon nitrogen starvation (as opposed to zygotic meiosis, in which haploids conjugate and immediately undergo meiosis, the scenario preferred by fission yeast and referred to throughout this paper unless specified), we observe a high number of cells with contacts throughout meiotic prophase. These long-lived contacts are associated with a bipolar spindle formation frequency of 100%. This explains the reduction in overall bipolar spindle formation in zygotic versus azygotic *bqt1Δ* meiosis (bipolar spindles are seen in 40% of the former and 60% of the latter; Fig. 1 E). As azygotic meiotic cells are smaller than zygotes, an intuitive expectation is that the likelihood of contacts between SPBs and chromatin is increased simply by crowding (Fig. 1 F). Correspondingly, we noticed a twofold increase in spindle defects in *bqt1Δ* meiocytes grown in liquid media, which are larger than those grown on solid media. An inverse relationship between cell size and proper spindle formation is also suggested by the results of bouquet loss in the cell size mutants *wee1-50* and *cdc25-22* (*Cdc25-C532Y*). Although loss of *bqt1* in the smaller *wee1-50* cells conferred only a slight reduction in sporulation efficiency (~90% asci with four equally sized spores), bouquet loss in the larger *cdc25-22* cells yields four healthy-looking spores in only 20% of asci. Thus, the rate of aberrant spindle formation in a *bqt1Δ* setting correlates with cell size, most likely because of the enhanced probability of prophase chromatin–SPB contacts in smaller cells.

The foregoing observations implicate chromatin–SPB contacts in successful meiotic spindle formation. To define the nature of these contacts, we visualized the centromere via Mis6, an inner kinetochore component that remains at centromeres throughout meiotic prophase (Asakawa et al., 2005; Fig. 2, A–C; and Video 3). In a *WT* setting, centromeres dissociate from the SPB once the telomeres arrive at the onset of meiotic prophase (Fig. 2 A; Klutstein et al., 2015). The bulk of centromeres also dissociate from the SPB at the onset of prophase in a bouquet-deficient setting, leaving the fluctuating SPB to stray far from the chromatin mass, which remains static in the middle of the cell. Despite this separation of the SPB from the main chromatin mass, it always remains associated with the NM throughout prophase (see below). The SPB settles at the end of prophase in *bqt1Δ* cells as it does in *WT* cells, even though it subsequently fails to nucleate stable spindles (Fig. 2 B). As noted above, a considerable proportion of *bqt1Δ* meiocytes displays a segment of chromatin associated with the SPB during prophase along with proper bipolar spindles. Strikingly, in 72% of these cases the chromatin segment contains a clear Mis6 signal, indicating that the centromere itself contacts the SPB (Figs. 2, C and D). On the rare occasions where contact appears to be mediated by a noncentromeric region, the contact tends to be shorter (Fig. 2 E);

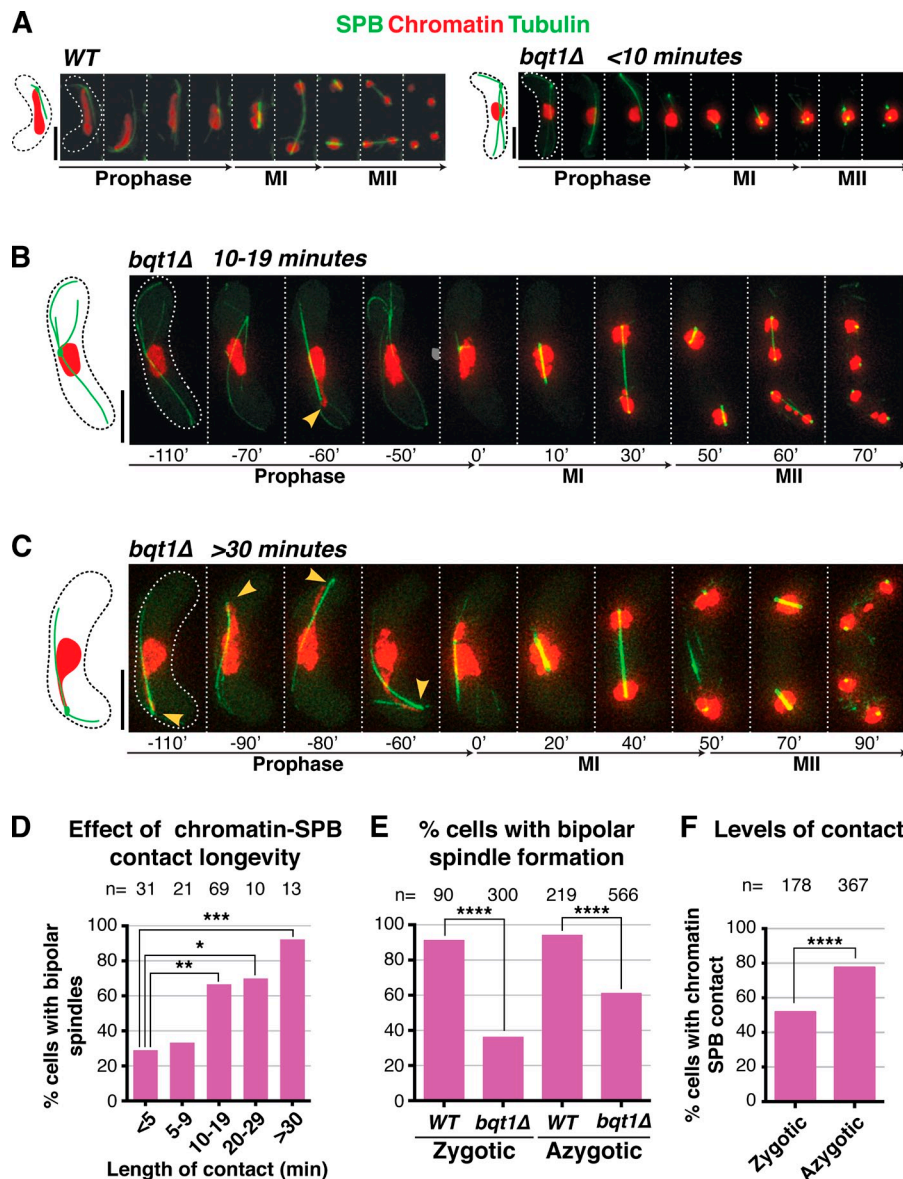


Figure 1. Rescue of *bqt1Δ* spindle defect by prophase chromatin-SPB contacts. (A–C) Frames from films of meiocytes carrying Hht1-mRFP (histone H3 tagged at one of the two endogenous *hht1*⁺ loci; Chromatin), Sid4-GFP (endogenously tagged; SPB), and ectopically expressed GFP-Atb2 (*nmt1* promoter controlled; Tubulin). Numbering indicates meiotic progression in minutes; *t* = 0 is just before spindle formation. Bars, 5 μm. (A) A *bqt1Δ* meiocyte with <10-min contact displays a monopolar MI spindle and unstable MII spindles. (B and C) *bqt1Δ* cells with 10–19-min and >30-min chromatin-SPB contact (yellow arrowheads) show proper spindles at MI and MII. (D) Quantitation of effect of chromatin-SPB contact duration on bipolar MI spindle formation. *n* is the total number of cells scored in eight independent experiments; data were subject to Fisher's exact test: ***, 0.0001 < *P* < 0.001; **, 0.001 < *P* < 0.01; *, 0.01 < *P* < 0.05. All cells scored for A–D of this figure are more extensively analyzed in Fig. S1 (C and D). (E) Bipolar spindle formation is more frequent in azygotic than zygotic *bqt1Δ* meiosis. *n* is the total number of cells scored from at least two (WT) and more than eight (*bqt1Δ*) independent experiments in a range of strain backgrounds; ****, *P* < 0.0001. (F) Comparison of chromatin-SPB contact frequency in zygotic and azygotic meiosis. *n* is the total number of cells scored from >3 (WT) and >10 (*bqt1Δ*) independent experiments (for chromatin-SPB contact data) and ≥5 (WT and *bqt1Δ*) independent experiments (for centromere-SPB contact data).

moreover, as the Mis6 signal is often faint, the lack of a clear signal cannot be used to definitively rule out centromeric localization. In line with the correlation between chromatin-SPB contact duration and proper spindle formation (Fig. 1, B–D), we observe a correlation between Mis6-SPB contact duration and proper spindle formation (Fig. 2, F and G; and Fig. S1, A–F).

Observation of the centromeric histone H3 variant Cnp1 (Fig. 2 H) again reveals that centromeres mediate the chromatin-SPB contacts that rescue spindle formation in bouquet-deficient settings. Likewise, a higher frequency of centromere-SPB interactions is seen in azygotic than zygotic *bqt1Δ* meiosis. Therefore, prophase centromere-SPB contacts predict improved spindle formation in *bqt1Δ* meiosis.

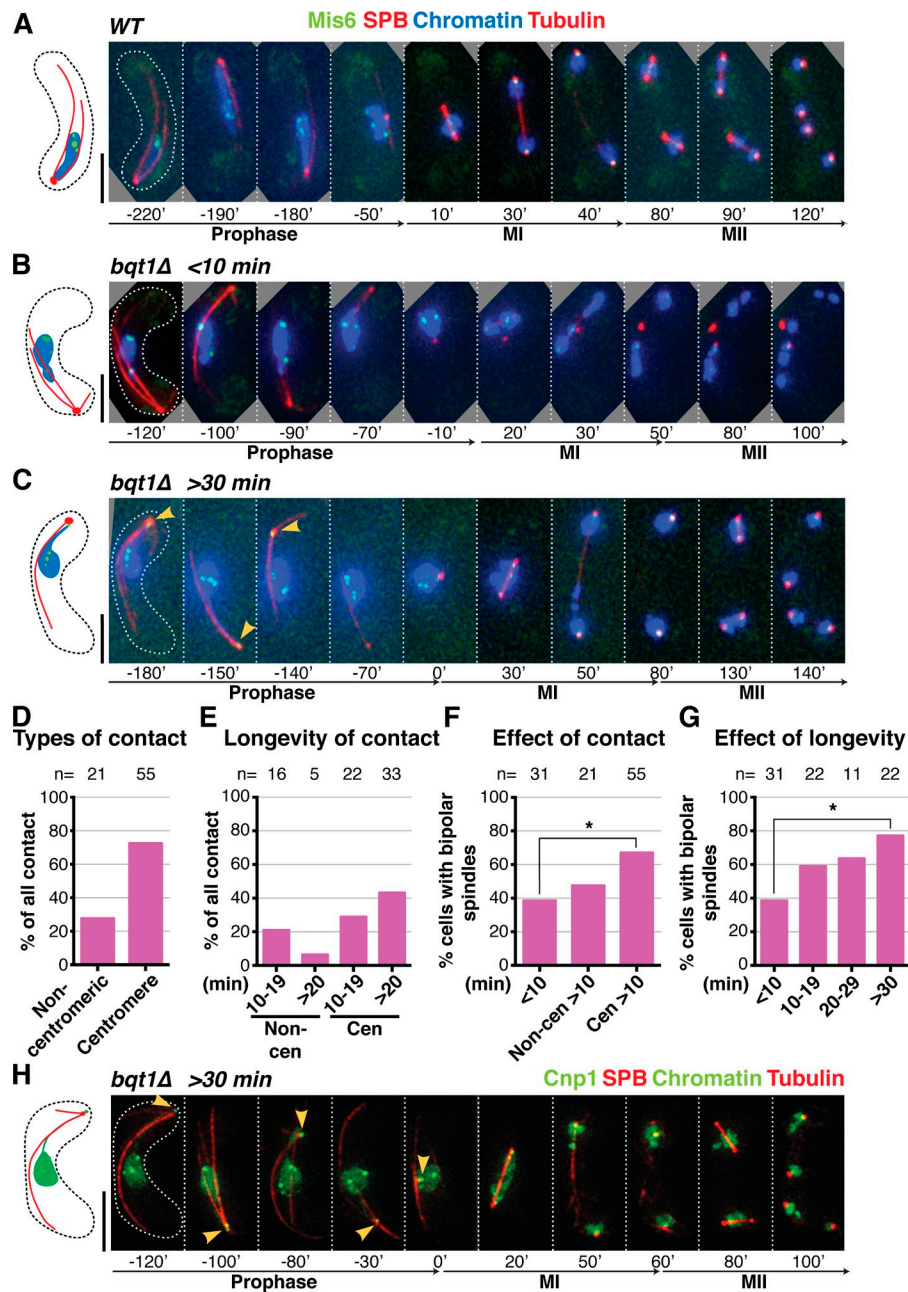
Forced long-lived centromere-SPB contacts fully rescue *bqt1Δ* spindles

To further substantiate the idea that long-lived centromere-SPB contacts confer proper spindle formation, we sought to induce a complete rescue of the *bqt1Δ* spindle defect by maintaining

centromeres at the SPB throughout meiotic prophase. To achieve this, we used the GFP-binding protein (GBP; Rothbauer et al., 2006) fused to the C terminus of endogenous Bqt1 to recruit GFP-tagged Mis6 (and hence, centromeres) to the SPB in a *rap1Δ* setting (Fig. 3 A). Indeed, coexpression of Mis6-GFP and Bqt1-GFP results in efficient recruitment such that at least one centromere is seen at the SPB throughout prophase in nearly all cells. In this forced centromere-SPB interaction scenario, nearly 100% bipolar MI spindle formation is achieved despite the absence of Rap1 (and therefore the absence of the bouquet; Fig. 3, B–F; and Video 4). Conversely, in those rare Mis6-GFP Bqt1-GFP cells lacking Mis6-Bqt1 contact, the spindle is defective. Hence, forced long-lived centromere-SPB contacts fully rescue spindle defects in bouquet-deficient settings.

An independent approach to assessing the result of “throughout” centromere-SPB contacts in bouquet-deficient settings is provided by meiocytes in which horsetail movements are compromised via deletion of *dhc1*⁺ (which encodes the dynein heavy chain) or *hrs1*⁺ (which encodes a meiosis-specific

Figure 2. Centromeres mediate the chromatin–SPB contacts that rescue *bqt1Δ* spindle defects. (A–C and H) Frames from films of meocytes carrying Hht1-CFP (at a single endogenous locus as in Fig. 1; Chromatin), Sid4-mCherry (SPB), ectopically expressed mCherry-Atb2 (Tubulin), and endogenously tagged Mis6-GFP (A–G) or Cnp1-GFP (ectopically expressed under control of endogenous promoter; H). Bars, 5 μ m. (A) In WT cells, centromeres do not localize to the SPB during meiotic prophase. (B) *bqt1Δ* cell showing <10-min centromere–SPB contact during prophase followed by failed spindle formation. (C and H) A centromere–SPB contact lasting >30 min (indicated by yellow arrowheads) is followed by bipolar spindle formation. (D) Levels of centromeric versus noncentromeric chromatin–SPB contact during *bqt1Δ* meiotic prophase. (E) Longevity of centromeric versus noncentromeric contacts. (F) Levels of *bqt1Δ* bipolar MI spindle formation seen in cells with the specified types of chromatin–SPB contact. The percentage of bipolar spindle formation seen in noncentromeric >10-min contact (Non-cen >10 min) is likely an overestimate caused by the faintness of Mis6-GFP signals. (G) Proper spindle formation is quantified as a function of centromere–SPB contact duration. *n* is the number of cells scored in 14 independent experiments. All cells scored for this figure are more extensively analyzed in Fig. S1 (E and F). *, 0.01 < *P* < 0.05.

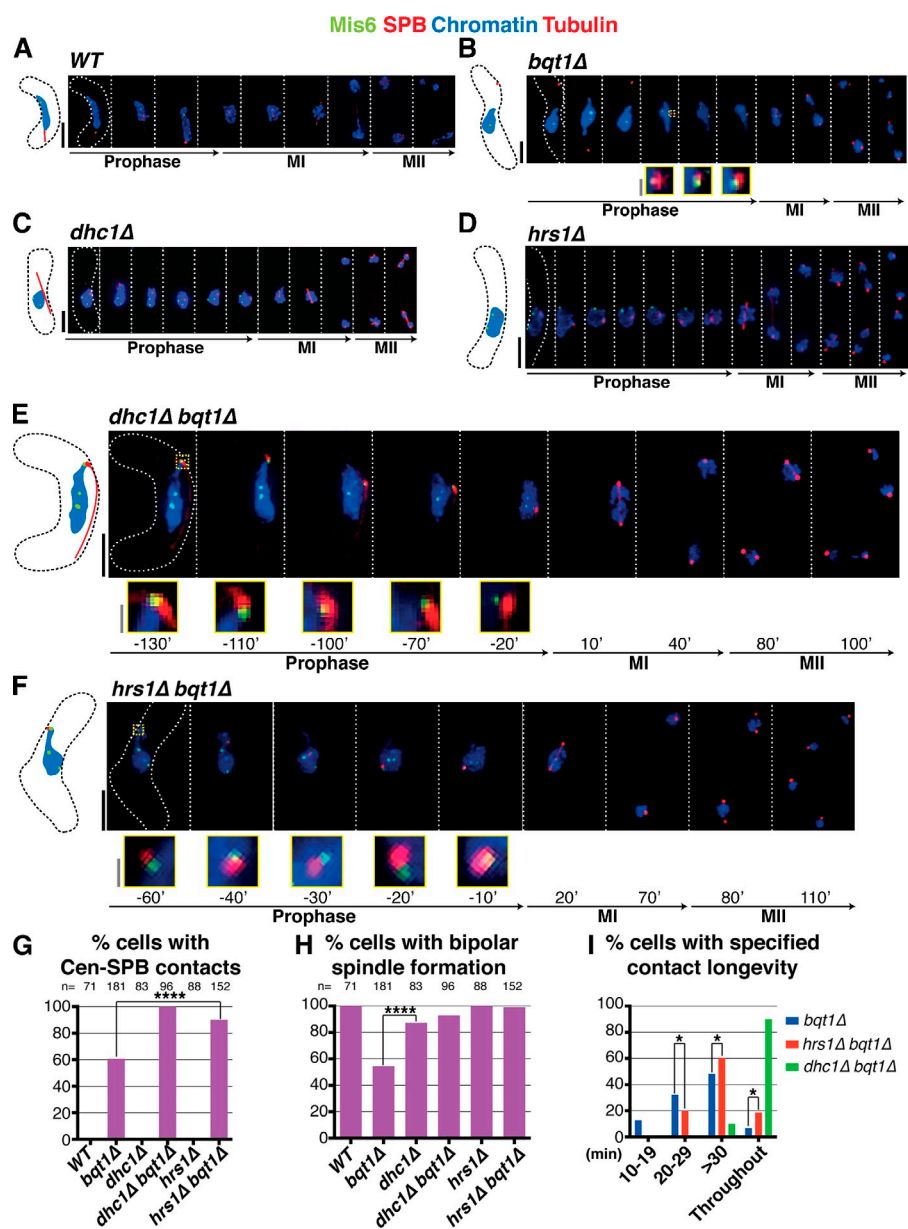


SPB component required for horsetail movement; Yamamoto et al., 1999; Saito et al., 2005; Tanaka et al., 2005). We previously observed that *dhc1Δ bqt1Δ* meocytes suffer defective spindle formation reminiscent of *bqt1Δ* single mutant meocytes (Tomita and Cooper, 2007). However, if we revisit these analyses excluding all *dhc1Δ bqt1Δ* meocytes displaying karyogamy defects, we find that the majority of *dhc1Δ bqt1Δ* meocytes show proper bipolar spindle formation; this has also been observed by others (Chikashige et al., 2014). Hence, the loss of vigorous nuclear movement suppresses *bqt1Δ* spindle defects in those cells displaying robust karyogamy. Complete centromere release from the meiotic SPB occurs only upon the onset of horsetail nuclear movements (Klutstein et al., 2015), suggesting that disruption of such movement could confer maintenance of stable centromere–SPB contact in *bqt1Δ* mutants, thus

explaining the restored bipolar spindle formation in *dhc1Δ bqt1Δ* cells. Hence, we investigated centromere–SPB association in these backgrounds. Whereas *dhc1Δ* and *hrs1Δ* single mutant meocytes show normal centromere release during prophase (Fig. 4, C and D), *dhc1Δ bqt1Δ* and *hrs1Δ bqt1Δ* meocytes show incomplete centromere release, with all cells displaying at least one centromere–SPB contact throughout prophase (Fig. 4, E–G; Fig. S1 G; and Video 5; Klutstein et al., 2015). These “throughout” centromere–SPB contacts can account for proper bipolar spindle formation (Fig. 4 H).

Although the persistence of centromere–SPB interactions upon cessation of prophase SPB movement can explain the suppression of *bqt1Δ* spindle defects by *dhc1* and *hrs1* deletion, the loss of movement by itself could also contribute to rescued spindle assembly; indeed, such spindle rescue in a related

Figure 4. Loss of Dhc1 or Hrs1 confers long-lived centromere–SPB contact in *bqt1Δ* zygotes. (A–F) All labels are as in Fig 2 with Mis6-GFP marking the centromere. Bars: (black) 5 μ m; (gray) 1 μ m. (A) Centromeres are absent from the SPB during horsetail movement in WT meiotic prophase. (B) Chromatin occasionally follows the SPB during prophase in *bqt1Δ* cells; sporadic centromere–SPB contacts (inset and magnified in yellow) confer bipolar spindle formation. (C and D) In *dhc1Δ bqt1+* and *hrs1Δ bqt1+* zygotes, vigorous SPB movement is abolished but centromeres are released from the SPB. (E and F) In contrast, *dhc1Δ bqt1Δ* and *hrs1Δ bqt1Δ* zygotes maintain at least one centromere at the SPB throughout prophase, ensuring normal spindle formation. (G) Although only around 60% of *bqt1Δ* cells show centromere–SPB contacts, all *dhc1Δ bqt1Δ* and the majority of *hrs1Δ bqt1Δ* cells show this interaction. No such contacts are observed in WT, *dhc1Δ*, or *hrs1Δ* cells. The analyses use Mis6-GFP as a centromere marker; the faintness of this marker explains the appearance of cells in which no centromere–SPB contact can be seen in a *hrs1Δ bqt1Δ* setting. Using the brighter Swi6-GFP as a marker for centromeres, we observe contact throughout in all cells (not depicted). (H) Quantitation shows complete restoration of *bqt1Δ* spindle formation by *hrs1+* or *dhc1+* deletion. *n* is the total number of cells scored from greater than six independent experiments. ****, $P < 0.0001$. (I) Categorization of zygotes according to longevity of their centromere–SPB contacts. The majority of *dhc1Δ bqt1Δ* cells show “throughout” (entire length of horsetail stage) prophase centromere–SPB contacts. All cells scored for this figure are more extensively analyzed in Fig. S1 G. The data shown are from three independent experiments analyzing >50 cells each. *, $0.01 < P < 0.05$.



with the SPB (Fig. 6, B–E; and Fig. S1, H–J). Hence, centromere size (which is largest for chromosome III and smallest for chromosome I) may influence SPB interactions; for example, a larger centromere may persist longer at the SPB during its horsetail movements or may have a greater chance of reencountering the SPB once dissociated. Current studies aim to decipher the basis for these preferential interactions.

Substitution of telomeres by centromeres is independent of *Clr4*, *Dcr1*, *Nuf2*, and *Csi1*

What feature of telomeres and centromeres allows both to promote meiotic spindle formation after prophase SPB contact? Their shared status as major heterochromatic regions prompted us to ask whether the histone methyltransferase *Clr4* and/or the RNAi pathway component *Dcr1* are required. Double mutant *bqt1Δ clr4Δ* and *bqt1Δ dcr1Δ* meocytes show levels of spindle defects similar to those of *bqt1Δ* single mutants and, as in *bqt1Δ*

meiocytes, the double mutants maintain a tight correlation between chromatin–SPB contacts and proper spindle formation (Fig. S2). Therefore, *Clr4* and *Dcr1* are dispensable for rescue of the *bqt1Δ* spindle defect by chromatin–SPB contact.

The control experiments assessing single *clr4Δ* and *dcr1Δ* mutants initially surprised us by revealing proper spindle formation (Fig. S2, A, C, and E) despite previous observations, using FISH to mark the telomere-adjacent rDNA region, that these single mutants sustain bouquet defects (Hall et al., 2003; Tuzon et al., 2004). Using live analysis to monitor telomeres via Taz1, we find that bouquet formation is largely intact in the absence of *Clr4* or *Dcr1*. However, instances in which multiple Taz1 foci are seen during meiotic prophase are more frequent in some *clr4Δ* and *dcr1Δ* clones, suggesting that the bouquet is less stable in these settings and more prone to disruption by fixation and FISH (unpublished data). Moreover, as SPB contact with a single telomere stretch is sufficient to confer spindle

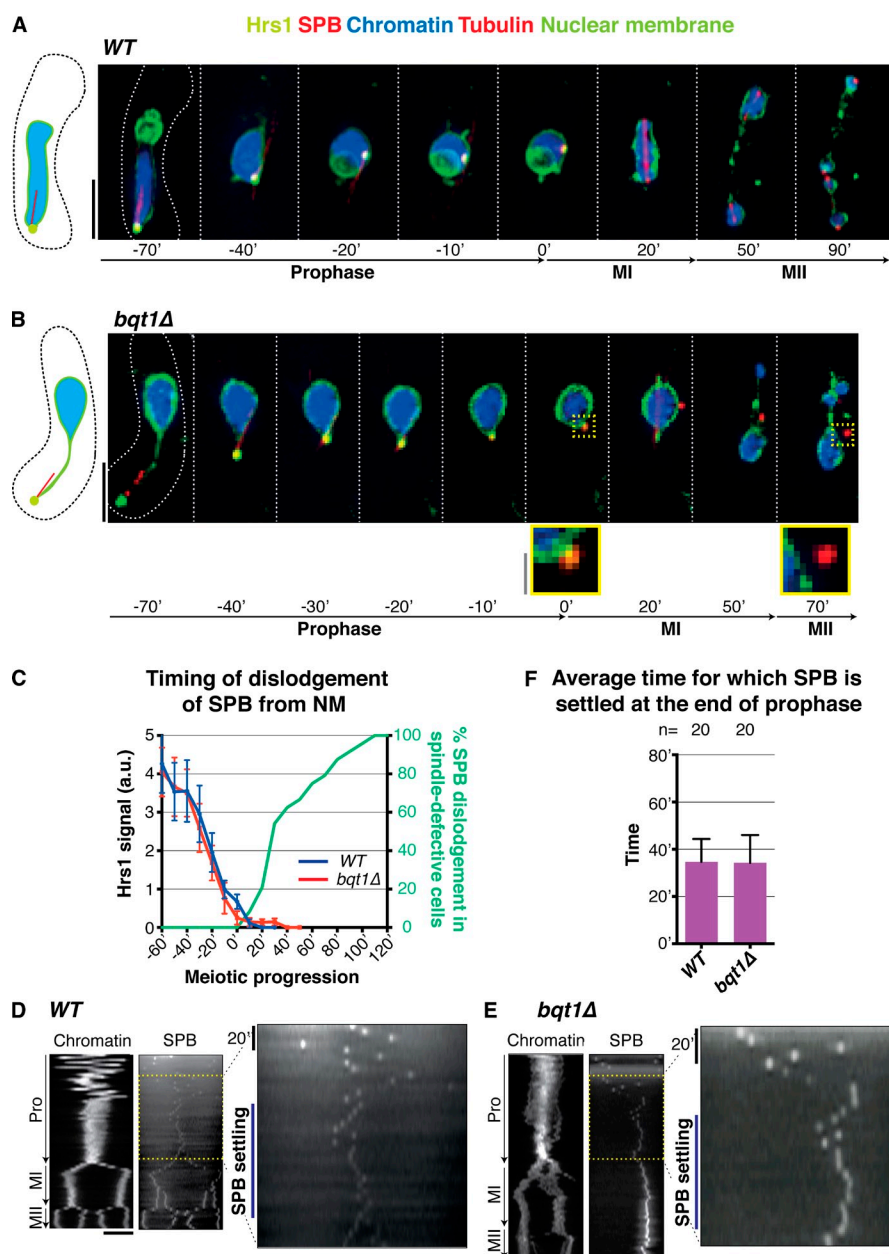


Figure 5. SPB settling occurs regardless of bouquet status. (A and B) Frames from films of meocytes with endogenously GFP-tagged Hrs1 and *nmt1*-controlled Ish1-GFP (to visualize the NM) along with the indicated markers (as in Fig. 2). Bars: (black) 5 μ m; (gray) 1 μ m. (A) In WT meocytes, the SPB colocalizes with the NM throughout meiosis. (B) In *bqt1Δ* meocytes, the SPB detaches from the NM only after SPB movement ceases, i.e., upon disappearance of Hrs1-GFP ($t = 0'$). (C) Quantitation and timing of phenotypes shown in A and B from three independent experiments analyzing 30 cells for each strain. Note that dislodgement of the SPB from the NM is never observed in WT meocytes. SPBs of *bqt1Δ* cells dissociate from the NM only after Hrs1 signal has disappeared. (D and E) Kymographs of Hht1-CFP (Chromatin) and Sid4-mCherry (SPB) during prophase, MI, and MII. The SPB settling phase (yellow) is shown magnified. The data shown are from a single representative experiment out of >10 repeats. (F) Time (in minutes) for which SPB (as visualized via Hrs1-GFP) settles after prophase. n is the total number of cells scored from greater than six independent experiments. Error bars show the mean SD.

formation (Tomita et al., 2013), cells suffering only a partial bouquet disruption would not suffer perturbed spindle formation.

Hence, the ability to control meiotic spindle formation may be independent of heterochromaticity. However, the possibility remains that some self-propagating feature downstream of Clr4 or Dcr1 function is required for SPB control in a scenario analogous to centromere assembly itself; although adjacent heterochromatin is required for establishment of centromeres on naive sequences, this heterochromatin is dispensable for the inheritance of preformed centromeres (Karpen and Allshire, 1997; Folco et al., 2008).

To explore the roles of factors known to affect centromere–SPB interactions during mitotic cell cycles, we examined Nuf2, an outer kinetochore component whose meiotic prophase-specific disappearance correlates with disassociation of centromeres from the SPB, and Csi1, a protein that binds the SUN domain protein Sad1 and is required for full centromere–SPB

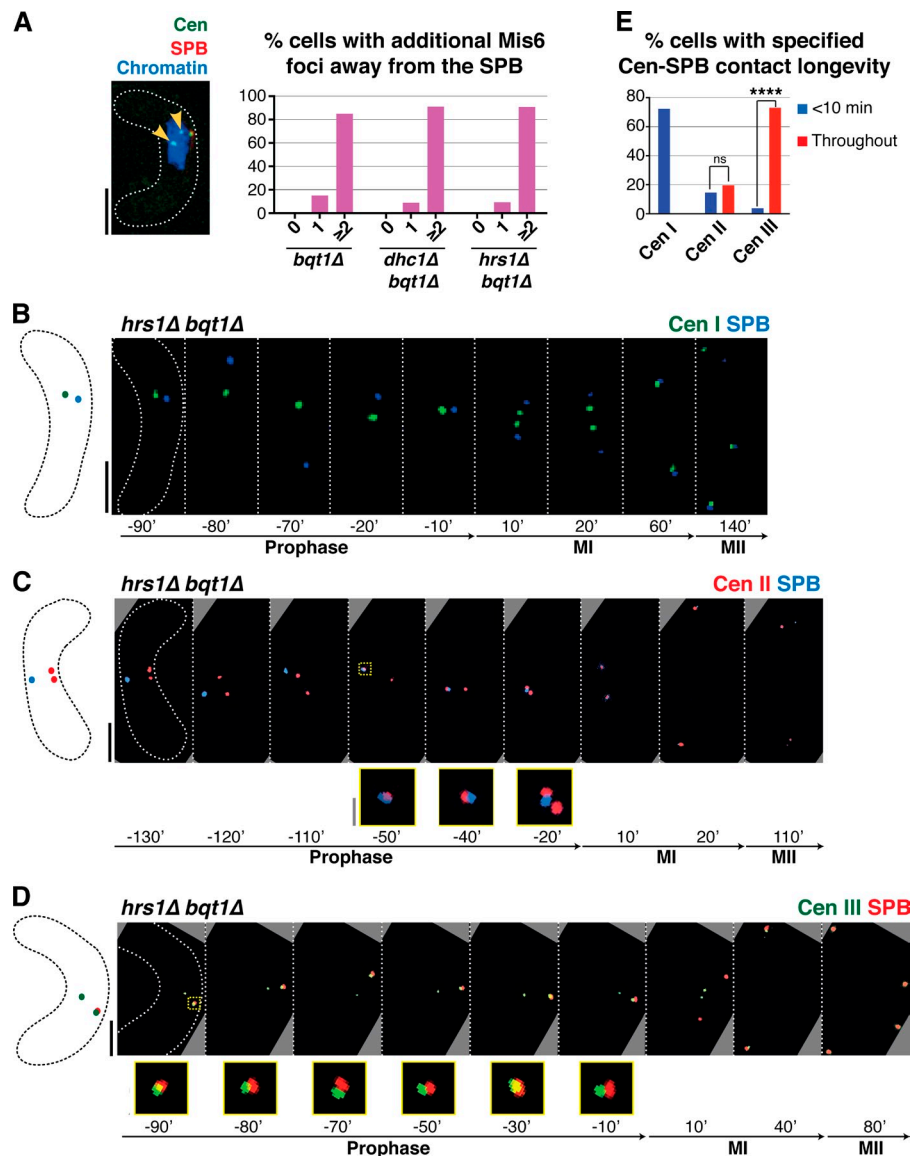
association during mitotic interphase (Asakawa et al., 2005; Hou et al., 2012). As seen in WT meiosis (Asakawa et al., 2005), Nuf2 disappears from the kinetochore upon meiotic entry in *bqt1Δ* cells, regardless of their centromere–SPB contact status (unpublished data); hence, Nuf2 does not appear to mediate the ability of centromeres to contact the *bqt1Δ* SPB. Similarly, the ability of the centromere to bind the SPB in a bouquet-deficient background is independent of Csi1 (Fig. S3). Future work aims to identify the specific feature of the centromere that mediates stable interaction with the meiotic SPB.

Noncentromeric chromatin regions are less able than centromeres to restore *bqt1Δ* bipolar spindle formation

A key question is whether the centromere specificity of the chromatin contacts that rescue spindle formation stems from an

Figure 6. **Prophase centromere–SPB contacts in a *bqt1Δ* setting show a preference for *cenIII*.**

(A) In cells with centromere–SPB contacts, additional centromeric foci are observed away from the SPB. Arrowheads mark Mis6-GFP dots far from the SPB during *dhc1Δ bqt1Δ* prophase. Quantitation is shown to the right. More than 100 cells were scored in five independent experiments. (B–D) Series of frames of films of *hrs1Δ bqt1Δ* meiosis. Numbering as in Fig 1; the SPB is viewed via endogenously tagged Sad1-CFP. Bars: (black) 5 μ m; (gray) 1 μ m. (B) The centromere of chromosome I is visualized via a LacI-GFP-bound *lys1⁺-lacO* array. (C) The centromere of chromosome II is visualized via a TetR-bound *cnt2-tetO* array. (D) The centromere of chromosome III was followed via a LacI-bound *ade6-lacO* array. In these cells, Sad1 is endogenously tagged with mRFP. (E) Collated centromere–SPB interactions. SPB interactions with *cenIII* are more frequent and longer lasting than those with *cenI* or *cenII*; moreover, *cenIII*–SPB interactions are more frequent and longer than *cenI*–SPB interactions. More than five independent experiments were performed. All cells scored for this figure are more extensively analyzed in Fig. S1 (H–J). ****, $P < 0.0001$.



ability uniquely shared by centromeres and telomeres to successfully modify SPB-associated factors or whether all chromatin possesses this SPB-modifying capacity but centromeres and telomeres have a higher propensity to associate with the SPB. Although contacts of >20 min between noncentromeric regions and the SPB are too rare to lend firm conclusions, we find that for a given SPB contact duration, the chances of *bqt1Δ* spindle rescue by noncentromeric chromatin are lower than that for centromeres (Fig. 2 F). To address this issue directly, we used Bqt1-GBP in combination with *lacO/I-GFP* arrays inserted at centromeric versus noncentromeric sites, theoretically conferring the respective recruitment of the two sites to the meiotic prophase SPB (Fig. S4). As expected, centromere-proximal *lacO/I-GFP* Bqt1-GBP ensures successful recruitment of centromeric chromatin to the SPB for long periods in *rap1Δ* meocytes, and this contact confers vastly improved bipolar spindle formation (Fig. 7, A–C). In contrast, arm-proximal *lacO/I-GFP* Bqt1-GBP fails to confer improved *rap1Δ* bipolar spindle formation (Fig. 7, B–E), suggesting that contact between the SPB

and a random chromatin site is insufficient to promote spindle formation. However, the efficacy of SPB recruitment by Bqt1-GBP differs between the two *lacO/I-GFP*-tagged loci. For CEN-proximal *lacO/I-GFP*, one bright focus remains associated with Bqt1-GBP at the prophase SPB, whereas another stays with the nuclear bulk; the two foci presumably represent the two homologues, which remain largely unpaired in bouquet-deficient settings (Ding et al., 2004; Fig. 7 A). In contrast, arm-associated *cut3-lacO/I-GFP* appears less tightly associated with Bqt1-GBP, as both bright GFP foci are often seen in the nuclear bulk with only a diffuse GFP halo appearing near the SPB, presumably representing excess free LacI molecules (Fig. 7 E). We presume that the enhanced SPB recruitment of centromere-proximal sites stems from reinforcement of GFP-GBP-based recruitment by the natural affinity of centromeric chromatin for the SPB. Nonetheless, despite the caveat that euchromatic sequences are recruited less efficiently than centromeric sequences to the SPB using this system, those instances of clear recruitment suggest that chromosome arm regions are less able than centromeres to confer

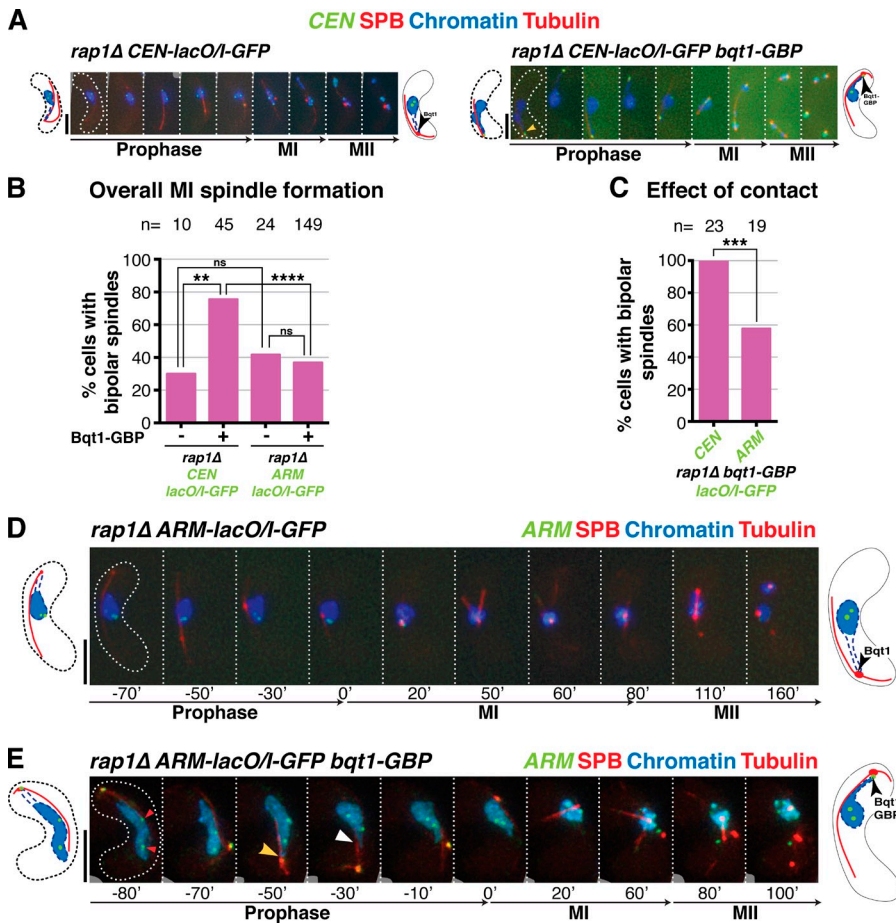


Figure 7. CEN-proximal regions show greater affinity for the SPB, and greater ability to rescue spindle formation, than ARM-proximal regions. (A, D, and E) Series of frames of films of meiocytes harboring the tags detailed in Fig. S4; numbering as in Fig. 1. Bars, 5 μ m. (A) *rap1Δ* meiotic spindle defect is rescued by forcing long-lived interaction between CEN-proximal region and SPB during meiotic prophase. (B) Quantitation of overall bipolar meiotic spindle formation in specified backgrounds. (C) Quantitation of effect of specified contact on bipolar spindle formation, scoring only those cells with contact >50 min. For meiocytes harboring *cut3⁺-lacO/I-GFP*, cells with one GFP focus ($n = 4$) or two foci in nucleoplasm were scored if and only if a clear GFP focus was present at the SPB. n is the total number of cells scored; data were subject to Fisher's exact test: ****, $P < 0.0001$; ***, $0.0001 < P < 0.001$; **, $0.001 < P < 0.01$. (D) As expected, *rap1Δ* cells with no chromatin contact have defective meiotic spindles. (E) Example of a *rap1Δ cut3⁺-lacO/I-GFP bqt1-GBP* zygote. One GFP focus is seen at the SPB and two are seen within the bulk of the nucleus (left, red arrowheads), indicating incomplete recruitment of *cut3* locus to the SPB. Yellow arrowhead indicates clear chromatin-SPB contacts; white arrowhead indicates occasions of less clear contact, in which the nucleus appears to poke out in the direction of the SPB but chromatin markers are not clearly visible.

proper spindle formation upon contact. Hence, centromeres and telomeres have both a greater propensity to interact with the SPB and a stronger ability to modify its behavior.

Centromeres and telomeres share the ability to confer increased levels of Sad1 at the SPB

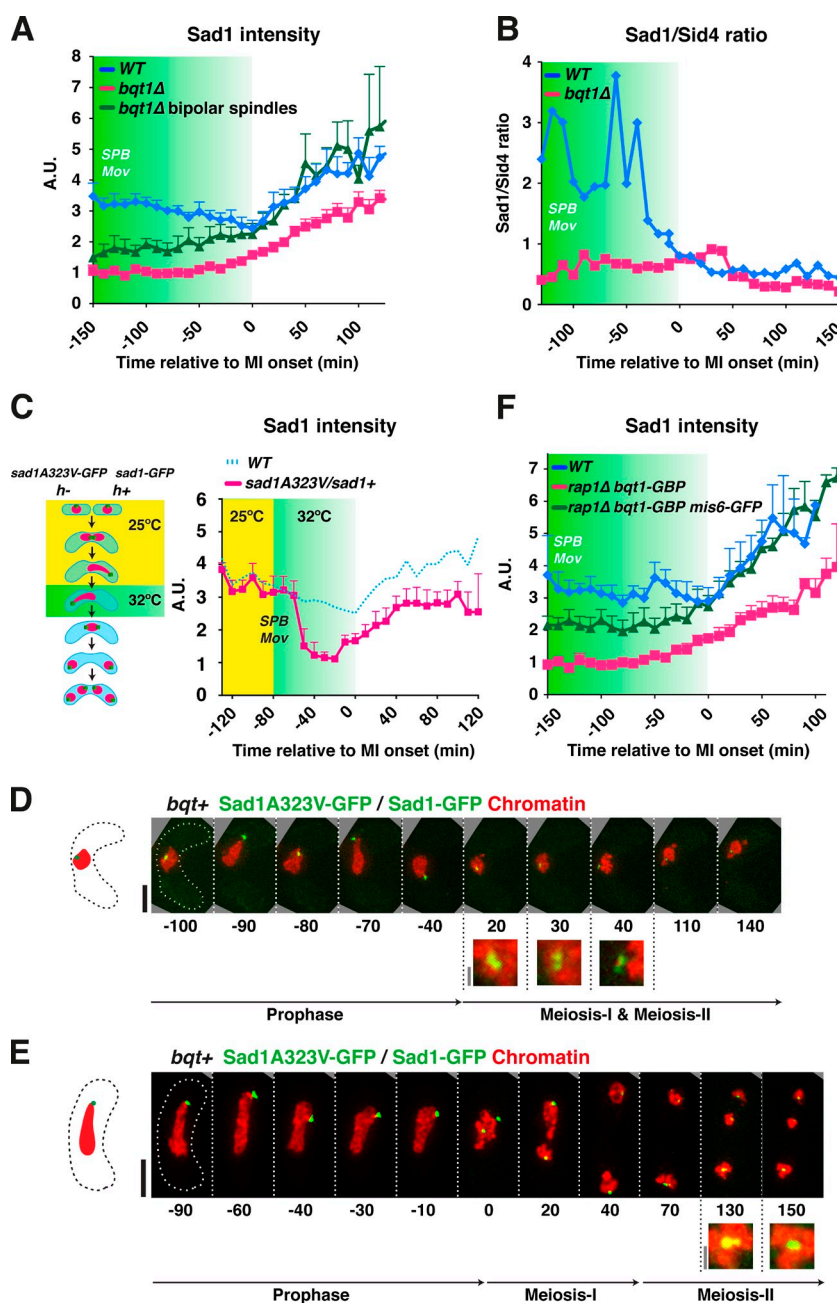
The foregoing results indicate that telomeres and centromeres share the ability to confer proper SPB behavior and spindle formation. To investigate the molecular underpinnings of this shared ability, we analyzed the behavior of Sad1, the SUN domain inner NM protein that connects centromeres and telomeres with the NM and is crucial for spindle formation (Hagan and Yanagida, 1995). We followed the dynamics of endogenously GFP-tagged Sad1 in live *WT* and *bqt1Δ* meiocytes and quantified focal Sad1 intensity throughout meiosis (see Materials and methods). Interestingly, the signal intensity of Sad1-GFP at the SPB is significantly reduced in those *bqt1Δ* meiocytes displaying defective spindle formation (Fig. 8, A and B). This reduction of Sad1 level is consistent and stable throughout prophase at all positions along the trajectory of horsetail movement, as well as at MI and MII.

To test the idea that Sad1 levels at the SPB are a relevant bouquet-controlled parameter for promoting spindle formation, we designed a system to test for meiotic haploinsufficiency of *sad1⁺* using the *ts* allele *sad1.1* (Hagan and Yanagida, 1995),

which contains an alanine to valine substitution at position 323 in the N-terminal region of the SUN domain. To follow Sad1-A323V behavior by live microscopy, we inserted a C-terminal GFP tag and confirmed that growth is temperature sensitive (Fig. S5 A). In heterozygous *sad1-GFP/sad1A323V-GFP* strains, Sad1 levels are reduced to ~50% of *WT* levels within an hour after shift to the nonpermissive temperature of 32°C (Fig. S5). We allowed *sad1-GFP/sad1A323V-GFP* meiocytes to undergo normal bouquet formation at 25°C and then switched the temperature to 32°C, filming throughout (Fig. 8 C). After the temperature shift-induced reduction in Sad1 levels at the SPB, chromosome separation fails in a manner reminiscent of that seen upon bouquet disruption (Fig. 8, D and E). These observations confirm that a threshold level of Sad1 at the SPB must be attained to ensure successful meiosis.

Notably, we found that in those *bqt1Δ* meiocytes that form proper bipolar spindles, Sad1 intensities at MI are similar to those in *WT* meiocytes (Fig. 8 A, green line). This observation not only reinforces the correlation between Sad1 accumulation at the SPB and proper spindle formation, but also suggests that centromeres and telomeres share the ability to promote enhanced Sad1 accumulation at the SPB. To explore this idea explicitly, we forced the interaction between centromeres and the SPB in the absence of the bouquet, using the Bqt1-GBP/Mis6-GFP system described above, and asked whether this forced interaction guarantees Sad1 accumulation. Remarkably,

Figure 8. Sad1 accumulation at the SPB is promoted by telomeres and centromeres. (A) Mean Sad1-GFP signal intensities at the SPB through meiosis were quantified in 19 WT meiotic cells, 21 *bqt1Δ* meiotic cells showing spindle defects, and 19 *bqt1Δ* meiotic cells with proper spindle formation. The data shown are from >10 independent experiments. 0 min represents the onset of MI and error bars represent standard deviations. Green shading indicates the period of horsetail SPB movement. (B) Sad1-GFP/Sid4-mCherry intensity ratios are shown for the same cells quantified in A, as Sid4 intensity profiles through meiosis are identical in WT and bouquet-defective meiotic cells (unpublished data). (C, left) Schematic of the strategy used to achieve an approximate halving of Sad1 level. A diploid constructed by crossing *h⁺ sad1-GFP hht1-mRFP* and *h⁻ sad1-A323V-GFP hht1-mRFP* was meiotically induced. Once prophase horsetail movement commenced, the temperature was switched to 32°C to inactivate Sad1-A323V; the subsequent meiosis was filmed to assess spindle formation. (right) Sad1-GFP intensities, from 10 meiotic cells for each genotype shown, are plotted over time relative to MI onset. Yellow shading indicates the time points taken at 25°C; the subsequent time points were taken 32°C. (D and E) Series of frames of Sad1-GFP/Sad1-A323V-GFP meiotic cells showing SPB problems when the temperature was switched to 32°C. Bars: (black) 5 μm; (gray) 1 μm. (F) Quantitation of Sad1-mCherry intensity levels in the strains indicated. Greater than 10 meiotic cells are represented for each genotype.



the GBP-GFP-induced centromere–SPB interaction resulted in levels of Sad1 that increased through meiotic prophase and achieved WT levels at MI and MII (Fig. 8 F). Hence, both accidental and forced centromere–SPB contacts rescue spindle formation in bouquet-deficient cells at least in part by conferring accumulation of Sad1 at the SPB.

Discussion

The 50% penetrance of spindle defects in bouquet-deficient meiosis indicated the existence of a redundant pathway by which spindle formation could be stimulated in the absence of telomere–SPB contact. Here we show that centromere–SPB interactions provide this alternative pathway. Hence, centromeres and telomeres are interchangeable in this respect, sharing an

ability not possessed by other chromatin regions to contact the NM just beneath the SPB, in turn promoting Sad1 accumulation and spindle nucleation.

Meiotic spindle formation requires several compositional changes within the SPB during the preceding prophase, as several proteins that show constitutive SPB localization during mitotic cell cycles are evicted in early prophase and then actively stockpiled at the SPB before MI onset (Jin et al., 2002; Ohta et al., 2012). Remarkably, this SPB maturation process remains unaltered in a bouquet-deficient background, regardless of whether a given *bqt1Δ* meiotic cell is destined to achieve successful spindle formation (unpublished data). In contrast, Sad1 accumulation and SPB insertion into the NM at MI onset are compromised in the absence of the bouquet (this work; unpublished data). Importantly, those long-lived prophase centromere–SPB contacts

that rescue subsequent meiotic spindle formation also rescue Sad1 accumulation. Therefore, the functional interchangeability between centromeres and telomeres likely resides in their ability to interact with and accrue Sad1 at the SPB, thereby ensuring spindle nucleation (Fig. 9, A–C). Interestingly, simple overexpression of Sad1 is not sufficient to promote its accumulation at the SPB; instead, overexpressed Sad1 spreads around the NM (Hagan and Yanagida, 1995; unpublished data). Hence, the bouquet- or centromere-stimulated SPB accumulation of Sad1 must involve some conformational change or modification of Sad1 or of the local NM milieu that allows its retention beneath the SPB, rather than just the mobilization of non-SPB-associated Sad1 from distal regions of the NM. The idea of chromatin-stimulated SUN domain protein modification has precedent in studies of *Caenorhabditis elegans* SUN1, whose phosphorylation during meiotic prophase is promoted by contact with the pairing centers, unique chromosome regions that localize near but not at telomeres and initiate homologue pairing. Pairing center-mediated SUN1 phosphorylation is in turn required for SUN1- and dynein-driven chromosome movements and full meiotic progression. These phospho-modifications depend not only on pairing center contact but also on the polo and Chk-2 kinases (Sato et al., 2009; Harper et al., 2011; Labella et al., 2011). In mouse, the meiosis-specific telomere binding protein TERB1 promotes association of telomeres with the NM and actively recruits the SUN–KASH complex to telomere–NM attachment sites (Shibuya et al., 2014), again highlighting a dynamic interplay between SUN domain protein function and the chromatin sites with which it interacts. However, it remains unknown whether worm or mouse chromosome–SUN interactions impact spindle assembly as they do in fission yeast.

Although the factors that confer prophase interactions between telomeres and the SPB are known, the mechanism by which centromeres interact with Sad1 to afford its accumulation at the SPB in a bouquet-deficient setting remains enigmatic. Centromeres are generally released from the SUN–KASH–SPB (SKS) linkage regardless of whether the bouquet forms (Tomita and Cooper, 2007; this work); nonetheless, we observe a single centromere associating with the SKS for at least 10 min during prophase in over half of zygotic *bqt1Δ* meocytes. Hence, we propose that although centromere release initiates upon dissolution of the outer kinetochore (Asakawa et al., 2005) and occurs in earnest upon the onset of horsetail nuclear movements (Klutstein et al., 2015), the absence of the telomere bouquet liberates the SKS from steric hindrance, providing centromeres with the opportunity to reassociate with the SKS at any point during prophase. The likelihood of this situation is increased dramatically when both bouquet formation and nuclear movement are disrupted (*bqt1Δ dhc1Δ*). Moreover, centromeres clearly have a higher propensity than noncentromeric regions to interact stably with the SPB. Our efforts to define the molecular underpinnings of this propensity have thus far ruled out essential roles for Ctr4 and Dcr1, both of which are required to maintain pericentric heterochromatin; hence, we expect that elements of the centromere that can be maintained in the absence of methylated H3-K9, most likely the Cnp1-packaged centromeric central core, confer SKS interaction. Indeed, simultaneous

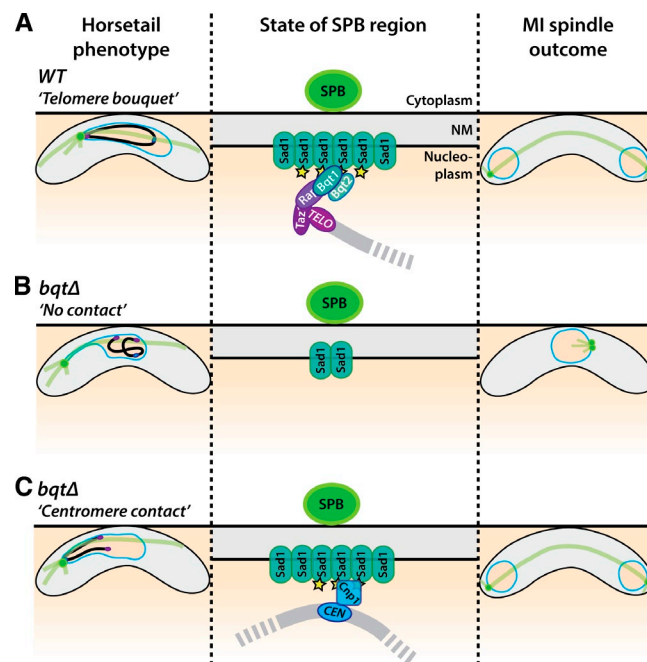


Figure 9. Centromere–telomere interchangeability in promoting meiotic spindle formation. Meiotic progression is represented from left to right. (A) In WT meocytes, the movement of telomeres to the SPB promotes modification of Sad1 (yellow stars) or the NM surrounding Sad1, in turn promoting Sad1 accumulation and ensuring bipolar spindle formation. (B) In *bqt1Δ* meocytes with no chromatin–SKS contact, Sad1 accumulation fails, as does spindle nucleation. (C) In *bqt1Δ* meocytes with centromere–SPB contact, Sad1 concentrates beneath the SPB as in WT.

disruption of *clr4* and *clr3* (which encodes a histone deacetylase) in the *bqt1Δ* setting leads to reduced levels of centromere–SPB contact and defective spindle formation (unpublished data), consistent with the effects of such double gene disruption on centromeric central core Cnp1 maintenance. Therefore, centromere identity by itself likely dictates the ability of centromeres to associate with the meiotic prophase SPB and substitute for telomeres in promoting spindle formation.

Although Csi1 is known to mediate central core–SPB interactions in mitotic interphase (Hou et al., 2012), the fact that some centromeres retain interphase SPB association in the absence of Csi1 (Hou et al., 2012) implies the existence of further uncharacterized components involved in this interaction; the dispensability of Csi1 for the rescuing centromere–SPB contacts we observe in *bqt1Δ* meocytes further underscores the existence of such additional factors. In considering factors that might confer SKS-modifying ability, Rec8 and Moa1 (a meiosis-specific cohesin subunit and stimulator of monopolar attachment, respectively [Yokobayashi and Watanabe, 2005; Sakuno et al., 2009]) arose as viable candidates, as both are recruited to the centromeric central core in a H3-K9 methylation-independent manner; however, both are dispensable for centromeric rescue of *bqt1Δ* meiotic spindle formation (unpublished data). Hence, some other central core-associated (presumably Cnp1-dependent) feature imparts SKS modification ability. The supremacy of CenIII in terms of *bqt1Δ* spindle-rescuing ability could be explained by its longer central core domain.

Layered upon the issue of how meiotic centromeres associate stably with the SKS in the absence of the bouquet is the question of what feature shared between telomeres and centromeres endows these distinct chromosome sites with SPB regulatory capacity. The fact that a single telomere repeat stretch (Tomita et al., 2013) or a single centromere (Fig. 6) is sufficient to ensure bipolar spindle formation rules out the possibility that the relevant property involves the clustering of multiple such regions; moreover, our observation that forced interaction between *lac* arrays in euchromatin and the SKS fail to confer proper spindle formation argues against the possibility that repeats by themselves possess SKS-modifying ability. Conceivably, this ability is inherent to stretches of chromatin with some specific torsional or condensation-related property of centromeres and telomeres. It will be fascinating to determine the features of these regions that imparts their interchangeability.

The finding that centromeres can substitute for telomeres in controlling meiotic spindle formation may have important implications for mitotic cell cycles as well. Indeed, the well-established mitotic interphase contact between centromeres and the SKS suggests the tantalizing possibility that centromeres control mitotic SPB behavior in a manner reminiscent of the role of meiotic telomeres. Such mitotic chromatin-based control could provide an extra layer of cell cycle regulation, perhaps ensuring a dependency of spindle assembly upon the completion of specific chromosomal events (like DNA replication, chromatin assembly, or chromatin repair). Intriguingly, the origin recognition complex replication activation proteins have been shown to interact with human centrosomes and regulate the centrosome cycle, perhaps comprising a related mode by which chromosomal and centrosomal events are coupled (Prasanth et al., 2004; Hemerly et al., 2009).

Our discovery of an interchangeable role of centromeres and telomeres is consistent with the notion that centromeres derived from telomeres in parallel with the evolution of a complex cytoskeleton during the transition from a single circular genotype to multiple, linear, eukaryotic chromosomes (Méndez-Lago et al., 2009). Whereas the observation of a shared role for centromere and telomeres in promoting spindle formation is unprecedented, the use of centromeres in one organism to perform functions assumed by telomeres in another organism is prominently illustrated by the meiotic centromere clustering seen in *Drosophila melanogaster* oocytes that is thought to be analogous to the bouquet in facilitating homologue pairing (Takeo and Hawley, 2012). Centromere clustering is also thought to augment early meiotic chromosome sorting processes in polyploid plants (Wen et al., 2012). Moreover, a role for chromatin in controlling spindle formation is likely to be conserved in higher eukaryotes, especially as chromatin has been shown to promote spindle nucleation in *Xenopus laevis* extracts (Heald et al., 1997). Centromeres and telomeres may have coevolved to share features that enhance this spindle-promoting ability.

Materials and methods

Strains and media

Strains are listed in Table S1. Gene deletions/tag insertions were created as described previously (Grimm et al., 1988; Tomita and Cooper, 2007).

Insertions of mCherry-Atb2 at the *aur1* locus (Hashida-Okado et al., 1998) used pYC19-mCherry-atb2 (Nakamura et al., 2011) provided by T. Toda (Cancer Research UK, London, UK). The vector for GFP binding protein tagging (Rothbauer et al., 2006) was provided by M. Sato (Waseda University, Tokyo, Japan).

Media were as described previously (Moreno et al., 1991). Cells grown in YES at 32°C were plated on malt extract at 30°C to induce meiosis and analyzed 5–7 h later (live analysis).

Live analysis

Cells were adhered to 35-mm glass culture dishes (MatTek Corporation) using 0.2 mg/ml of soybean lectin (Sigma-Aldrich) and immersed in EMM-N (with required supplements \pm 15 mM thiamine). Time-lapse imaging was performed at 27°C in an Environmental Chamber with a DeltaVision Spectris (Applied Precision) comprising a widefield inverted epifluorescence microscope (IX70; Olympus), a 100 \times NA 1.4 oil immersion objective (UPlanSapo; Olympus), and a charge coupled device CoolSnap HQ camera (Photometrics). Images were acquired over 26 focal planes at a 0.35- μ m step size with frames taken every 10 min for 7 h. Images were deconvolved (enhanced ratio method) and combined into a 2D image using the maximum intensity projection setting for analysis using SoftWorx (Applied Precision). Sid4-GFP and Atb2-GFP were captured with 0.2-s exposures per plane, Hht1-mRFP for 0.06 s/plane, Atb2-mCherry and Sid4-mCherry for 0.4 s/plane, Hht1-CFP for 0.2 s/plane, Mis6-GFP for 0.35 s/plane, and Cnp1-GFP and Swi6-GFP for 0.3 s/plane. When three fluorescent channels were imaged, a fast acquisition mode was used in which each Z plane was exposed to each wavelength sequentially.

SPB (Sad1 or Sid4) signal quantitation was performed using Volocity software on images acquired over 26 focal planes at a 0.35- μ m step size at each time point. Images were deconvolved (enhanced ratio method) and combined into a 2D image using SoftWorx. For each time point, the intensity of the area containing a given signal was quantified and that of an equivalent signal-free region within the same cell was subtracted; the resulting signal intensities were normalized to the mean intensity for one pixel of background outside the cell. Image processing and analysis were performed using Photoshop CS5.1 (Adobe).

Scoring criteria

To score contact categories (Fig. 1), only those cells observed for at least 40 min of meiotic prophase and through the meiotic divisions were included. For those zygotic meiotic cells in which karyogamy was observed, scoring began two frames after the completion of karyogamy. For all other zygotic cells, scoring began upon the start of live analysis. For azygotic cells, scoring began two frames after the first dramatic SPB fluctuation upon initiation of horsetail movement (once interphase microtubules depolymerized). To categorize contact duration, scoring was terminated two frames before MI spindle formation. Cells were categorized according to their longest single contact. In the *rap1 Δ mis6-GFP bqt1-GBP* background (Fig. 3), only those meiocytes with at least 50 min of contact were scored. Cells with defects in karyogamy or chromosome condensation, which occasionally stem from UV exposure during karyogamy regardless of genotype, were discarded. In strains harboring tagged histone H3 but no tagged centromere protein, frames in which the SPB was within bulk chromatin were discarded, as it was impossible to assign direct chromatin–SPB contacts. Spindles were scored as bipolar if separation of duplicated SPBs and subsequent elongation of a spindle separating the chromatin masses was seen. Fischer's exact test was performed as described previously (Agresti, 1992). The two-tail p-value was used.

A MATLAB script (see online supplemental material) was written to clearly display the range of contact lengths occurring in individual cells using vector diagrams (Fig. S1), enabling analysis of individual cells within the population according to their contact-to-spindle phenotypes.

Western blot analysis

Cells were collected by centrifugation, washed with Tris-HCl, pH 9.0, and resuspended in 20% TCA with PMSF (1 mM) and protease inhibitors mix (SetIII; EMD Millipore). After agitation with acid washed glass beads (Sigma-Aldrich), tubes were pierced at the bottom and samples were recovered by centrifugation. Beads were washed with 20% TCA with PMSF (1 mM) and protease inhibitors mix and centrifuged, and the final pellet was resuspended in LDS sample buffer (Invitrogen). All manipulations were performed at 4°C. Proteins were separated on NuPAGE 4–12% Bis-Tris acrylamide gradient gels with MOPS SDS running buffer (Invitrogen). Blots were probed anti-GFP antibody produced in rabbit (Sigma-Aldrich) or anti-Histone H2B antibody produced in rabbit (Sigma-Aldrich). Horseradish

peroxidase-conjugated anti-rabbit IgG (GE Healthcare) were used as secondary antibodies. Visualization was performed using the ECL Plus Western Blotting Detection System (GE Healthcare).

Online supplemental material

Fig. S1 shows single cell analysis of chromatin/centromere-SPB contacts during prophase in bouquet-deficient meiotic cells. Fig. S2 shows that the centromere-SPB contacts that rescue *bqt1Δ* spindle formation require neither Ctr4 nor Dcr1. Fig. S3 shows that these centromere-SPB interactions are also independent of Csi1. Fig. S4 shows that forced interactions between the SPB and centromere- or chromosome arm-proximal loci have no effect on meiotic progression in a bouquet-proficient background. Fig. S5 shows the analysis of Sad1 protein levels in *sad1⁺/sad1-A323V* cells. Table S1 shows the genotypes of the strains used in this work. The MATLAB script is the source code for the vector diagram in Fig. S1. Video 1 shows a *bqt1Δ* meiotic cell with no contact and a defective spindle. Video 2 shows a *bqt1Δ* meiotic cell with persistent chromatin-SPB contact showing bipolar spindle formation. Video 3 shows that the rescuing chromatin-SPB contact is mediated by the centromere. Video 4 shows that forced centromere-SPB contact ensures bipolar spindle formation. Video 5 shows that loss of nuclear movement leads to centromere-SPB contact throughout and bipolar spindle formation. Online supplemental material is available at <http://www.jcb.org/cgi/content/full/jcb.201409058/DC1>.

We thank Cécile Bez for advice and discussion throughout this work, Alex Tournier for invaluable help with MATLAB analysis, Michael Lichten for comments on the manuscript, and our laboratory members for discussions. We thank Yasushi Hiraoka and Yuji Chikashige for sharing unpublished data and strains and Masamitsu Sato for strains.

This work was supported by the European Research Council, Cancer Research UK, the National Institutes of Health, and a European Molecular Biology Organization long-term fellowship to A. Fernández-Álvarez.

The authors declare no competing financial interests.

Submitted: 11 September 2014

Accepted: 9 January 2015

References

- Agresti, A. 1992. A survey of exact inference for contingency tables. *Stat. Sci.* 7:131–153. <http://dx.doi.org/10.1214/ss/1177011454>
- Artandi, S.E., and J.P. Cooper. 2009. Reverse transcribing the code for chromosome stability. *Mol. Cell.* 36:715–719. <http://dx.doi.org/10.1016/j.molcel.2009.11.030>
- Asakawa, H., A. Hayashi, T. Haraguchi, and Y. Hiraoka. 2005. Dissociation of the Nuf2-Ndc80 complex releases centromeres from the spindle-pole body during meiotic prophase in fission yeast. *Mol. Biol. Cell.* 16:2325–2338. <http://dx.doi.org/10.1091/mbc.E04-11-0996>
- Cheeseman, I.M., and A. Desai. 2008. Molecular architecture of the kinetochore-microtubule interface. *Nat. Rev. Mol. Cell Biol.* 9:33–46. <http://dx.doi.org/10.1038/nrm2310>
- Chikashige, Y., D.Q. Ding, H. Funabiki, T. Haraguchi, S. Mashiko, M. Yanagida, and Y. Hiraoka. 1994. Telomere-led premeiotic chromosome movement in fission yeast. *Science*. 264:270–273. <http://dx.doi.org/10.1126/science.8146661>
- Chikashige, Y., D.Q. Ding, Y. Imai, M. Yamamoto, T. Haraguchi, and Y. Hiraoka. 1997. Meiotic nuclear reorganization: switching the position of centromeres and telomeres in the fission yeast *Schizosaccharomyces pombe*. *EMBO J.* 16:193–202. <http://dx.doi.org/10.1093/emboj/16.1.193>
- Chikashige, Y., C. Tsutsumi, M. Yamane, K. Okamasa, T. Haraguchi, and Y. Hiraoka. 2006. Meiotic proteins bqt1 and bqt2 tether telomeres to form the bouquet arrangement of chromosomes. *Cell*. 125:59–69. <http://dx.doi.org/10.1016/j.cell.2006.01.048>
- Chikashige, Y., M. Yamane, K. Okamasa, C. Mori, N. Fukuta, A. Matsuda, T. Haraguchi, and Y. Hiraoka. 2014. Chromosomes rein back the spindle pole body during horsetail movement in fission yeast meiosis. *Cell Struct. Funct.* 39:93–100. <http://dx.doi.org/10.1247/csf.14007>
- Dehé, P.M., and J.P. Cooper. 2010. Fission yeast telomeres forecast the end of the crisis. *FEBS Lett.* 584:3725–3733. <http://dx.doi.org/10.1016/j.febslet.2010.07.045>
- de Lange, T. 2009. How telomeres solve the end-protection problem. *Science*. 326:948–952. <http://dx.doi.org/10.1126/science.1170633>
- Ding, D.Q., Y. Chikashige, T. Haraguchi, and Y. Hiraoka. 1998. Oscillatory nuclear movement in fission yeast meiotic prophase is driven by astral microtubules, as revealed by continuous observation of chromosomes and microtubules in living cells. *J. Cell Sci.* 111:701–712.
- Ding, D.Q., A. Yamamoto, T. Haraguchi, and Y. Hiraoka. 2004. Dynamics of homologous chromosome pairing during meiotic prophase in fission yeast. *Dev. Cell*. 6:329–341. [http://dx.doi.org/10.1016/S1534-5807\(04\)00059-0](http://dx.doi.org/10.1016/S1534-5807(04)00059-0)
- Folco, H.D., A.L. Pidoux, T. Urano, and R.C. Allshire. 2008. Heterochromatin and RNAi are required to establish CENP-A chromatin at centromeres. *Science*. 319:94–97. <http://dx.doi.org/10.1126/science.1150944>
- Greider, C.W., and E.H. Blackburn. 1985. Identification of a specific telomere terminal transferase activity in tetrahymena extracts. *Cell*. 43:405–413. [http://dx.doi.org/10.1016/0092-8674\(85\)90170-9](http://dx.doi.org/10.1016/0092-8674(85)90170-9)
- Grimm, C., J. Kohli, J. Murray, and K. Maundrell. 1988. Genetic engineering of *Schizosaccharomyces pombe*: A system for gene disruption and replacement using the *ura4* gene as a selectable marker. *Mol. Gen. Genet.* 215:81–86. <http://dx.doi.org/10.1007/BF00331307>
- Hagan, I., and M. Yanagida. 1995. The product of the spindle formation gene *sad1+* associates with the fission yeast spindle pole body and is essential for viability. *J. Cell Biol.* 129:1033–1047. <http://dx.doi.org/10.1083/jcb.129.4.1033>
- Hall, I.M., K. Noma, and S.I. Grewal. 2003. RNA interference machinery regulates chromosome dynamics during mitosis and meiosis in fission yeast. *Proc. Natl. Acad. Sci. USA*. 100:193–198. <http://dx.doi.org/10.1073/pnas.232688099>
- Harper, N.C., R. Rillo, S. Jover-Gil, Z.J. Assaf, N. Bhalla, and A.F. Dernburg. 2011. Pairing centers recruit a Polo-like kinase to orchestrate meiotic chromosome dynamics in *C. elegans*. *Dev. Cell*. 21:934–947. <http://dx.doi.org/10.1016/j.devcel.2011.09.001>
- Hashida-Okado, T., R. Yasumoto, M. Endo, K. Takesako, and I. Kato. 1998. Isolation and characterization of the aureobasidin A-resistant gene, *aur1R*, on *Schizosaccharomyces pombe*: roles of Aur1p+ in cell morphogenesis. *Curr. Genet.* 33:38–45. <http://dx.doi.org/10.1007/s002940050306>
- Heald, R., R. Tournebise, A. Habermann, E. Karsenti, and A. Hyman. 1997. Spindle assembly in *Xenopus* egg extracts: respective roles of centrosomes and microtubule self-organization. *J. Cell Biol.* 138:615–628. <http://dx.doi.org/10.1083/jcb.138.3.615>
- Hemerly, A.S., S.G. Prasanth, K. Siddiqui, and B. Stillman. 2009. Orc1 controls centriole and centrosome copy number in human cells. *Science*. 323:789–793. <http://dx.doi.org/10.1126/science.1166745>
- Hou, H., Z. Zhou, Y. Wang, J. Wang, S.P. Kallgren, T. Kurchuk, E.A. Miller, F. Chang, and S. Jia. 2012. Csi1 links centromeres to the nuclear envelope for centromere clustering. *J. Cell Biol.* 199:735–744.
- Jain, D., and J.P. Cooper. 2010. Telomeric strategies: means to an end. *Annu. Rev. Genet.* 44:243–269. <http://dx.doi.org/10.1146/annurev-genet-102108-134841>
- Jin, Y., S. Uzawa, and W.Z. Cande. 2002. Fission yeast mutants affecting telomere clustering and meiosis-specific spindle pole body integrity. *Genetics*. 160:861–876.
- Karpen, G.H., and R.C. Allshire. 1997. The case for epigenetic effects on centromere identity and function. *Trends Genet.* 13:489–496. [http://dx.doi.org/10.1016/S0168-9525\(97\)01298-5](http://dx.doi.org/10.1016/S0168-9525(97)01298-5)
- Klutstein, M., A. Fennell, A. Fernández-Álvarez, and J.P. Cooper. 2015. The telomere bouquet regulates meiotic centromere assembly. *Nat. Cell Biol.* In press.
- Labella, S., A. Woglar, V. Jantsch, and M. Zetka. 2011. Polo kinases establish links between meiotic chromosomes and cytoskeletal forces essential for homolog pairing. *Dev. Cell*. 21:948–958. <http://dx.doi.org/10.1016/j.devcel.2011.07.011>
- Méndez-Lago, M., J. Wild, S.L. Whitehead, A. Tracey, B. de Pablos, J. Rogers, W. Szybalski, and A. Villasante. 2009. Novel sequencing strategy for repetitive DNA in a *Drosophila* BAC clone reveals that the centromeric region of the Y chromosome evolved from a telomere. *Nucleic Acids Res.* 37:2264–2273. <http://dx.doi.org/10.1093/nar/gkp085>
- Moreno, S., A. Klar, and P. Nurse. 1991. Molecular genetic analysis of fission yeast *Schizosaccharomyces pombe*. *Methods Enzymol.* 194:795–823. [http://dx.doi.org/10.1016/0076-6879\(91\)94059-L](http://dx.doi.org/10.1016/0076-6879(91)94059-L)
- Nabetani, A., T. Koujin, C. Tsutsumi, T. Haraguchi, and Y. Hiraoka. 2001. A conserved protein, Nuf2, is implicated in connecting the centromere to the spindle during chromosome segregation: a link between the kinetochore function and the spindle checkpoint. *Chromosoma*. 110:322–334. <http://dx.doi.org/10.1007/s004120100153>
- Nakamura, Y., A. Arai, Y. Takebe, and M. Masuda. 2011. A chemical compound for controlled expression of nmt1-driven gene in the fission yeast *Schizosaccharomyces pombe*. *Anal. Biochem.* 412:159–164. <http://dx.doi.org/10.1016/j.ab.2011.01.039>
- Ohta, M., M. Sato, and M. Yamamoto. 2012. Spindle pole body components are reorganized during fission yeast meiosis. *Mol. Biol. Cell*. 23:1799–1811. <http://dx.doi.org/10.1091/mbc.E11-11-0951>

- Petronczki, M., M.F. Siomos, and K. Nasmyth. 2003. Un ménage à quatre: the molecular biology of chromosome segregation in meiosis. *Cell*. 112:423–440. [http://dx.doi.org/10.1016/S0092-8674\(03\)00083-7](http://dx.doi.org/10.1016/S0092-8674(03)00083-7)
- Prasanth, S.G., K.V. Prasanth, K. Siddiqui, D.L. Spector, and B. Stillman. 2004. Human Orc2 localizes to centrosomes, centromeres and heterochromatin during chromosome inheritance. *EMBO J.* 23:2651–2663. <http://dx.doi.org/10.1038/sj.emboj.7600255>
- Rothbauer, U., K. Zolghadr, S. Tillib, D. Nowak, L. Schermelleh, A. Gahl, N. Backmann, K. Conrath, S. Muyldermans, M.C. Cardoso, and H. Leonhardt. 2006. Targeting and tracing antigens in live cells with fluorescent nanobodies. *Nat. Methods*. 3:887–889. <http://dx.doi.org/10.1038/nmeth953>
- Saito, T.T., T. Tougan, D. Okuzaki, T. Kasama, and H. Nojima. 2005. Mcp6, a meiosis-specific coiled-coil protein of *Schizosaccharomyces pombe*, localizes to the spindle pole body and is required for horsetail movement and recombination. *J. Cell Sci.* 118:447–459. <http://dx.doi.org/10.1242/jcs.01629>
- Sakuno, T., K. Tada, and Y. Watanabe. 2009. Kinetochore geometry defined by cohesion within the centromere. *Nature*. 458:852–858. <http://dx.doi.org/10.1038/nature07876>
- Sato, A., B. Isaac, C.M. Phillips, R. Rillo, P.M. Carlton, D.J. Wynne, R.A. Kasad, and A.F. Dernburg. 2009. Cytoskeletal forces span the nuclear envelope to coordinate meiotic chromosome pairing and synapsis. *Cell*. 139:907–919. <http://dx.doi.org/10.1016/j.cell.2009.10.039>
- Scherthan, H. 2001. A bouquet makes ends meet. *Nat. Rev. Mol. Cell Biol.* 2:621–627. <http://dx.doi.org/10.1038/35085086>
- Shibuya, H., K. Ishiguro, and Y. Watanabe. 2014. The TRF1-binding protein TERB1 promotes chromosome movement and telomere rigidity in meiosis. *Nat. Cell Biol.* 16:145–156. <http://dx.doi.org/10.1038/ncb2896>
- Stimpson, K.M., and B.A. Sullivan. 2010. Epigenomics of centromere assembly and function. *Curr. Opin. Cell Biol.* 22:772–780. <http://dx.doi.org/10.1016/j.ceb.2010.07.002>
- Takeo, S., and R.S. Hawley. 2012. Rumors of its disassembly have been greatly exaggerated: the secret life of the synaptonemal complex at the centromeres. *PLoS Genet.* 8:e1002807. <http://dx.doi.org/10.1371/journal.pgen.1002807>
- Tanaka, K., T. Kohda, A. Yamashita, N. Nonaka, and M. Yamamoto. 2005. Hrs1p/Mcp6p on the meiotic SPB organizes astral microtubule arrays for oscillatory nuclear movement. *Curr. Biol.* 15:1479–1486. <http://dx.doi.org/10.1016/j.cub.2005.07.058>
- Tomita, K., and J.P. Cooper. 2007. The telomere bouquet controls the meiotic spindle. *Cell*. 130:113–126. <http://dx.doi.org/10.1016/j.cell.2007.05.024>
- Tomita, K., C. Bez, A. Fennell, and J.P. Cooper. 2013. A single internal telomere tract ensures meiotic spindle formation. *EMBO Rep.* 14:252–260. <http://dx.doi.org/10.1038/embor.2012.218>
- Tuzon, C.T., B. Borgstrom, D. Weilguny, R. Egel, J.P. Cooper, and O. Nielsen. 2004. The fission yeast heterochromatin protein Rik1 is required for telomere clustering during meiosis. *J. Cell Biol.* 165:759–765. <http://dx.doi.org/10.1083/jcb.200312061>
- Watanabe, Y. 2012. Geometry and force behind kinetochore orientation: lessons from meiosis. *Nat. Rev. Mol. Cell Biol.* 13:370–382. <http://dx.doi.org/10.1038/nrm3349>
- Wen, R., G. Moore, and P.J. Shaw. 2012. Centromeres cluster de novo at the beginning of meiosis in *Brachypodium distachyon*. *PLoS ONE*. 7:e44681. <http://dx.doi.org/10.1371/journal.pone.0044681>
- Yamamoto, A., R.R. West, J.R. McIntosh, and Y. Hiraoka. 1999. A cytoplasmic dynein heavy chain is required for oscillatory nuclear movement of meiotic prophase and efficient meiotic recombination in fission yeast. *J. Cell Biol.* 145:1233–1250. <http://dx.doi.org/10.1083/jcb.145.6.1233>
- Yanowitz, J. 2010. Meiosis: making a break for it. *Curr. Opin. Cell Biol.* 22:744–751. <http://dx.doi.org/10.1016/j.ceb.2010.08.016>
- Yokobayashi, S., and Y. Watanabe. 2005. The kinetochore protein Moa1 enables cohesion-mediated monopolar attachment at meiosis I. *Cell*. 123:803–817. <http://dx.doi.org/10.1016/j.cell.2005.09.013>
- Yoshida, M., S. Katsuyama, K. Tateho, H. Nakamura, J. Miyoshi, T. Ohba, H. Matsuhara, F. Miki, K. Okazaki, T. Haraguchi, et al. 2013. Microtubule-organizing center formation at telomeres induces meiotic telomere clustering. *J. Cell Biol.* 200:385–395. <http://dx.doi.org/10.1083/jcb.201207168>